10-10-2005

Hubble Space Telescope STIS spectroscopy of the Lyman-Alpha emission line in the central dominant galaxies in A426, A1795, and A2597: Constraints on clouds in the intracluster medium

Stefi Baum

Ari Laor

Christopher O'Dea

Recommended Citation
Astrophysical Journal 632 (2005) 122-136

The Astrophysical Journal, 632:122–136, 2005 October 10

HUBBLE SPACE TELESCOPE STIS SPECTROSCOPY OF THE Lyα EMISSION LINE IN THE CENTRAL DOMINANT GALAXIES IN A426, A1795, AND A2597: CONSTRAINTS ON CLOUDS IN THE INTRACLUSTER MEDIUM[1]

Stefi A. Baum
Center for Imaging Science, 54 Lomb Memorial Drive, Rochester Institute of Technology, Rochester NY 14623-5604

Ari Laor
Department of Physics, Technion-Israel Institute of Technology, Haifa, 32000, Israel

Christopher P. O'Dea
Department of Physics, 85 Lomb Memorial Drive, Rochester Institute of Technology, Rochester NY 14623-5603

and

Jennifer Mack and Anton M. Koekemoer
Space Telescope Science Institute,[2] 3700 San Martin Drive, Baltimore, MD 21218
Received 2005 March 14; accepted 2005 June 15

ABSTRACT

We report on *HST* STIS spectra of the Lyα emission in the central dominant galaxies in three rich clusters of galaxies. We find evidence for a population of clouds in the intracluster medium. We detect 10 Lyα absorption systems toward the nucleus of NGC 1275 with columns of $N(\mathrm{H\,I}) \sim 10^{12}$–$10^{14}$ cm^{-2}. These columns would not have been detected in the 21 cm line but are easily detected in the Lyα line. Most of the absorption features are located in the broad wings of the emission line. The detected absorption features are most consistent with associated nuclear absorption systems. There is very little nuclear absorption at the systemic velocity in NGC 1275 [feature 8 contains $N(\mathrm{H\,I}) \sim 3\times10^{12}$ cm^{-2}]. This implies that the large columns detected in the 21 cm line toward the parsec-scale radio source avoid the line of sight to the nucleus. This gas may be located in a circumnuclear disk or torus. We detect at least one and possibly two absorption features toward the extended Lyα in A426. We do not detect Lyα absorption toward the extended Lyα emission in A1795 and A2597 with upper limits $N(\mathrm{H\,I}) \sim 10^{13}$ cm^{-2} for optically thin absorbers. Our data constrain the covering factor of any high column density gas [$N(\mathrm{H\,I}) > 10^{15}$ cm^{-2}] in the ICM to be less than 25%. Our results suggest that the lack of observed intermediate-temperature gas is not explained by obscuration. In addition, the low columns of gas on $\sim$100 kpc scales in the ICM suggest that (1) the rate at which cold gas accumulates in the ICM on these scales is very low and (2) the dense nebulae in the central $\sim$10 kpc must have cooled or been deposited in situ.

Subject headings: cooling flows — galaxies: active — galaxies: clusters: individual (A426, A1795, A2597) — galaxies: ISM — ultraviolet: galaxies

1. INTRODUCTION

The hot $T \sim 10^7$–10^8 K X-ray–emitting gas is currently thought to constitute the bulk of the baryonic mass in rich clusters of galaxies. If substantial amounts of cold gas do exist in the intracluster medium (ICM), this would have important implications for our understanding of (1) cooling flows (how much mass do they deposit?), (2) the physics of the ICM (is it a multiphase medium like our ISM?), (3) the intracluster magnetic field (can it suppress conduction?), (4) galaxy formation and evolution (how important are winds and stripping?), and (5) Lyα forest systems (are they formed in clusters? e.g., Crawford et al. 1987).

There are several potential candidates for a population of cold clouds that might exist in the ICM of clusters of galaxies (e.g., Sarazin 1988): (1) Cold gas that has been removed from the individual galaxies, possibly by ram pressure stripping or by galaxy collisions (Soker et al. 1991; Sparks et al. 1989), (2) primordial clouds or protogalaxies that are currently falling into the cluster, and (3) clouds that condense from thermal instabilities in a cooling flow in the inner $\sim$100 kpc of the cluster center (e.g., Cowie & Binney 1977; Fabian & Nulsen 1977; Mathews & Bregman 1978; Fabian 1994). Mass accretion rates in cooling flows have been estimated to be in the range $\dot{m} \sim 10$–$100\ M_\odot\ \mathrm{yr}^{-1}$. If these accretion rates last for the lifetime of the cluster ($\sim 10^{10}$ yr), the accumulated mass in gas would be 10^{11}–$10^{12}\ M_\odot$. On the other hand, potential sinks and destructive processes for cold gas include (1) star formation (e.g., Allen 1995) and (2) heating and evaporation via thermal conduction, mixing layers, etc. (e.g., Sparks 1992; Böhringer & Fabian 1989), and shredding (e.g., Loewenstein & Fabian 1990).

X-ray spectroscopy with *XMM-Newton* and *Chandra* has failed to find evidence for gas at temperatures below about 1/3 of the cluster virial temperature (e.g., Kaastra et al. 2001; Tamura et al. 2001; Peterson et al. 2001, 2003). The limits on the luminosity of the intermediate-temperature gas imply reductions in the inferred mass accretion rates by factors of 5–10. One possibility

[1] Based on observations made with the NASA/ESA *Hubble Space Telescope*, obtained at the Space Telescope Science Institute, which is operated by the Association of Universities for Research in Astronomy, Inc., under NASA contract NAS 5-26555. These observations are associated with program 8107.

[2] Operated by the Association of Universities for Research in Astronomy, Inc., under contract NAS 5-26555 with the National Aeronautics and Space Administration.

TABLE 1
SOURCE PROPERTIES

Parameter	A426/NGC 1275	A1795	A2597
Second name	3C 84	4C 26.42	PKS B2322−123
V magnitude	12.5	14.2	15.8
Galactic $E(B-V)$	0.171	0.013	0.030
Observed Hα/Hβ	4.77	3.2	4.2 ± 0.1
Redshift	0.017559	0.06326	0.08220
Scale (kpc/arcsec)	0.33	1.12	1.42
1.4 GHz flux density (Jy)	21.2	1.0	2.0
Radio power $\log P_{1.4\,\mathrm{GHz}}$ (W Hz^{-1})	25.51	25.31	25.84

NOTES.—We adopt a Hubble constant of $H_0 = 75$ km s^{-1} Mpc^{-1} and a deceleration parameter of $q_0 = 0.0$. Balmer decrements are from Kent & Sargent (1979), Hu et al. (1985), and Voit & Donahue (1997), respectively.

is that there is a source of heat in the ICM (radio galaxies? e.g., Baum & O'Dea 1991; Tucker & David 1997; Soker et al. 2002; Böhringer et al. 2002) that halts the cooling of the gas. Alternately, it may be possible that the X-ray luminosity of the cooling gas is absorbed, with the luminosity finally emerging at another waveband (e.g., Fabian et al. 2001, 2002; Peterson et al. 2001). This raises the question of whether the required absorbing matter exists in these clusters.

Early X-ray observations indicated evidence for low-energy X-ray absorption in excess of what would be produced by the known Galactic column density of H I (e.g., White et al. 1991; Mushotzky 1992; Allen et al. 1993; Allen & Fabian 1994). White et al. (1991) suggested that this was evidence for the existence of a population of cold clouds with column density $N_{\mathrm{H}} \sim 10^{21}$–$10^{22}$ cm^{-2} and a covering factor of order unity. However, recent *Chandra* and *XMM-Newton* observations with greater sensitivity and spectral resolution have not confirmed the need for excess absorption. Current upper limits on the column density of hydrogen in the clusters are typically a few times 10^{20} cm^{-2} (e.g., Kaastra et al. 2001, 2004; Tamura et al. 2001; Peterson et al. 2001, 2003; Blanton et al. 2003; but see Ettori et al. 2002 for possible intrinsic absorption in A1795).

After a decade of nondetections, molecular gas has finally been detected in clusters other than A426 (Edge 2001). Roughly half the extreme cooling flow clusters surveyed by Edge exhibit CO corresponding to masses of molecular hydrogen in the range $\sim 10^9$–$10^{10}\ M_\odot$. Intensive searches for the 21 cm line of atomic hydrogen in both emission and absorption have placed limits on H I columns of $\lesssim 10^{19}$ cm^{-2} (e.g., Burns et al. 1981; Valentijn & Giovanelli 1982; McNamara et al. 1990; Jaffe 1991, 1992; Dwarakanath et al. 1994; O'Dea et al. 1995, 1998). H I absorption has been detected in only a few clusters (A426/3C 84, Crane et al. 1982; Jaffe 1990; Sijbring 1993; A780/Hydra A, Taylor 1996; A2597/PKS 2322−123, O'Dea et al. 1994; Taylor et al. 1999) with implied masses of atomic hydrogen in the range $\sim 10^7$–$10^8\ M_\odot$. The strong dominance of molecular relative to atomic gas in these clusters is in contrast to the situation in normal galaxies, where roughly ∼15% of the cold gas is thought to be in molecular form (e.g., Boselli et al. 2002); however, the bulk of the molecular gas in galaxies may be undetected (e.g., Allen et al. 1997).

The 21 cm limits on the H I column are subject to two caveats: (1) the limits depend linearly on the electron excitation temperature, which may be higher than previously thought; and (2) the absorbing gas may have a very small velocity dispersion, producing a very narrow saturated absorption line, and thus a lower absorption equivalent width than estimated for the optically thin case. The UV region provides a powerful but as yet not fully exploited probe of the ICM. The Lyα absorption cross section is $\gtrsim 10^7$ times larger than that of the 21 cm line (e.g., Bahcall & Ekers 1969; Laor 1997). In addition, it is not subject to the two caveats that affect the 21cm line, as (1) the absorption is practically independent of the gas temperature (the extremely short lifetime of the excited $n = 2$ level ensures that effectively all H I is in the ground level) and (2) significant absorption is expected even if the absorber has no velocity dispersion (the absorption occurs in the Lorentzian, or "damping," wings). Thus, Lyα is superior to the 21 cm line as a probe of the cold gas content of the ICM.

In fact, Koekemoer et al. (1998) presented *Hubble Space Telescope* Faint Object Spectograph (*HST* FOS) UV spectra of the quasar in the center of A1030 and placed limits on column densities in the range 10^{11}–10^{13} cm^{-2} for a wide range of molecular, atomic, and ionized species that may be associated with the ICM. Miller et al. (2002) obtained limits of 10^{12}–10^{13} cm^{-2} on column densities for several absorption lines (Fe II and Mg II) through lines of sight toward the outer parts of six clusters. Laor (1997) has used a low-resolution (∼250 km s^{-1}) *HST* FOS spectrum of the Lyα line in the center of the Perseus Cluster (published by Johnstone & Fabian 1995) to set an upper limit of $N_{\mathrm{H\,I}} \lesssim 4 \times 10^{17}$ cm^{-2}. It was clear that an improvement of several orders of magnitude in the constraints on the atomic hydrogen columns could be achieved by obtaining higher resolution spectra of the Lyα line.

In this paper we present medium-dispersion (20 km s^{-1}) *HST* Space Telescope Imaging Spectograph (STIS) long-slit spectroscopy of the Lyα line toward the central nebulae in three clusters, A426, A1795, and A2597. We report the discovery of Lyα absorption systems toward the nucleus and extended Lyα emission of NGC 1275. We discuss the nature and origin of these systems. We also place constraints on the properties of clouds in the ICM.

2. OBSERVATIONS AND RESULTS

The properties of the three central galaxies are summarized in Table 1. The *HST* STIS (Kimble et al. 1998) spectroscopic observations are summarized in Table 2. We observed with the far-UV Multianode Microchannel Array (MAMA) and the G140M grating centered on the redshifted Lyα emission line. Spectral and spatial pixel scales are 0.05 Å pixel^{-1} and 0.″029 pixel^{-1}, respectively. Spectral resolution is 1.6 pixels (0.08 Å) FWHM, which gives approximately 20 km s^{-1}. We used the 0.″1 slit to preserve our spectral and spatial resolution. We observed in TIME-TAG mode to allow us to reject data with high sky background.

TABLE 2
HST Spectroscopic Observations

Source (1)	Date (2)	Position Angle (deg) (3)	Exposure Time (s) (4)	Central λ (Å) (5)
A426.....	2000 Dec 5	100	4900	1222
A1795.....	2001 Mar 17	−158	4500	1272
A2597.....	2000 Nov 18	19	4300	1321

Notes.—Observations were obtained with the STIS FUV-MAMA and the G140M grating through the $5''.2 \times 0''.1$ slit under program 8107. TIME-TAG mode was used. Col. (1): Cluster name; col. (2): date of the observation; col. (3): slit position angle on the sky; col. (4): total exposure time; col. (5): central wavelength of the G140M grating.

We obtained "early acquisition" images of the Lyα emission line and the nearby far-UV continuum. These data are discussed by O'Dea et al. (2004). We used these images to select a position angle for the slit that maximized the amount of bright Lyα and/or far-ultraviolet (FUV) continuum in the slit. The locations of the slits are shown in Figures 1, 2, and 3. The data were reduced with the STIS pipeline using the best updated reference files.

The two-dimensional spectra are shown in Figures 4, 5, 6. We detect spatially extended Lyα emission in our spectra of all three sources. The fluxes for the extended emission are consistent with those derived from those locations in the UV images (O'Dea et al. 2004). In the A2597 spectrum, we also detect the geocoronal O I lines at 1302, 1305, and 1306 Å (Table 3). In A426 we detect a bright Lyα emission line with broad wings from the active nucleus. We do not see evidence for pointlike nuclear emission in A1795 or A2597.

3. ABSORPTION LINES TOWARD THE NUCLEUS OF NGC 1275

We detect 10 Lyα absorption systems toward the nucleus of NGC 1275 (3C 84; Fig. 7; Table 4). In order to determine the properties of each absorption system, we multiplied the observed spectrum by e^{τ_λ}, where τ_λ is the wavelength dependence of the optical depth of each system. The value of τ_λ is set by the center of the line, λ_0, the velocity dispersion parameter, and the H I column, through the standard Voigt profile calculations (e.g., Rybicki & Lightman 1979). We iterate over the values of these three parameters until the corrected spectrum appears featureless. We estimate the uncertainty in the column density and velocity dispersion to be at a level of 10%–30%. The wavelength uncertainty is generally set by the spectral resolution. This absorption correction procedure assumes absorption by a uniform screen. The implied column could be larger in case of partial obscuration (i.e., absorbing filaments that are smaller than the continuum source). The requirement that the Lyα damping wings are not broader than the observed absorption width provides a strict upper limit to the possible column. The two strongly damped systems correspond to Galactic absorption and to absorption by the infalling foreground system at 8200 km s^{-1}, also detected in H I. The column densities in the detected absorption lines are in the range $N(\mathrm{H\,I}) \sim 10^{12}$–$10^{14}$ cm^{-2}, and Doppler parameters are in the range $b \simeq 25$–70 km s^{-1}.

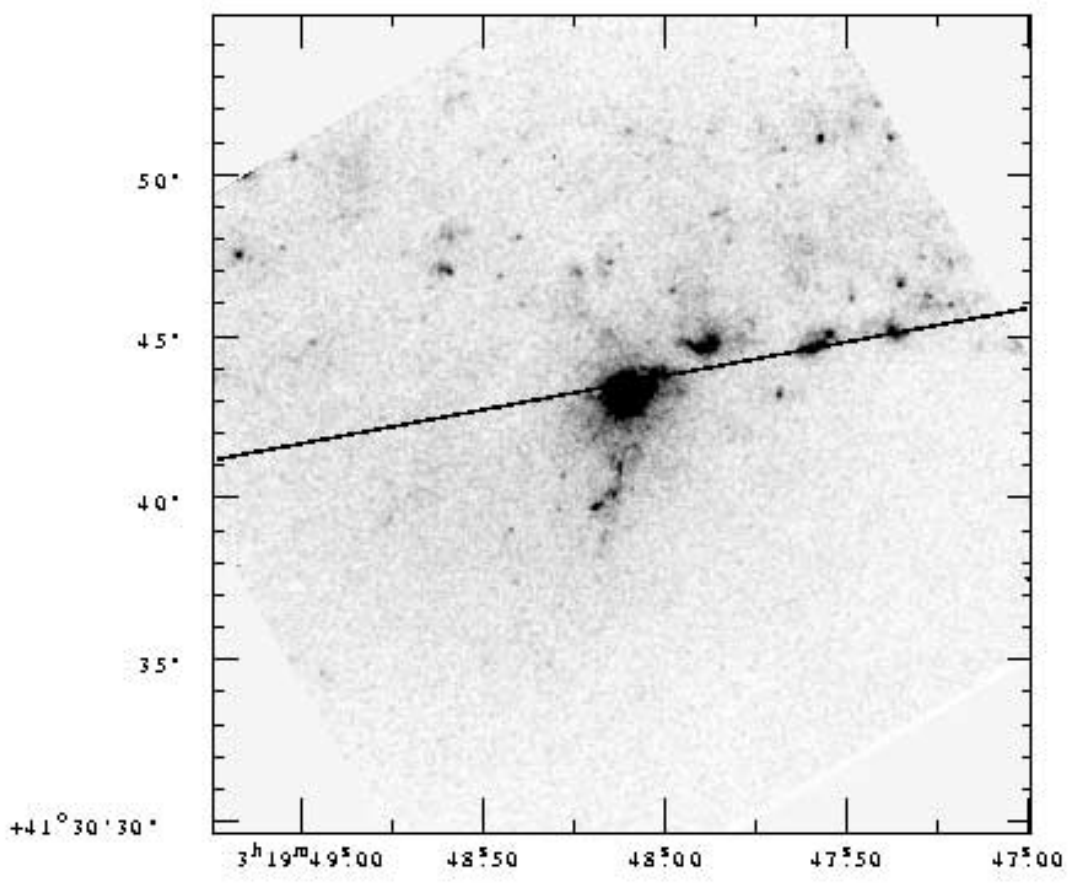

Fig. 1.—A426: STIS FUV-MAMA continuum image (from S. Baum et al. 2005, in preparation), showing the location of the slit position angle (100°). Positions are epoch J2000.0.

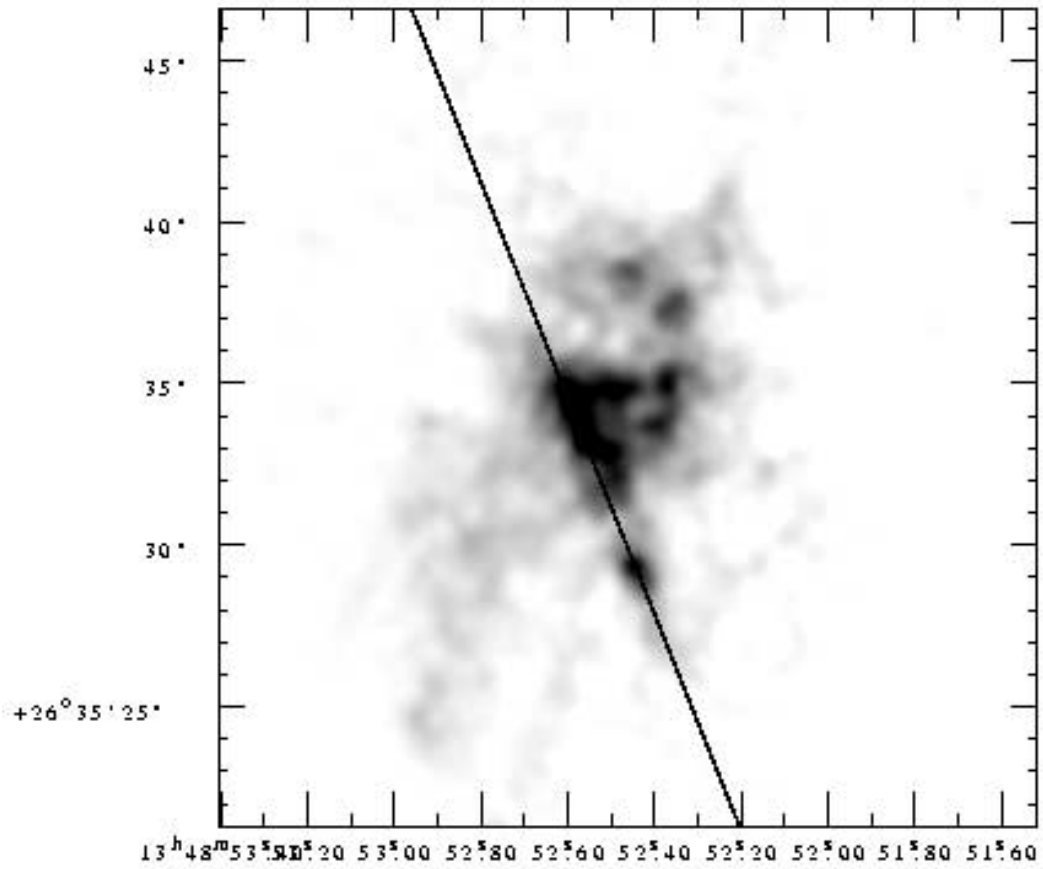

FIG. 2.—A1795: STIS FUV-MAMA Lyα image (O'Dea et al. 2004), showing location of the slit position angle (-158°). Positions are epoch J2000.0.

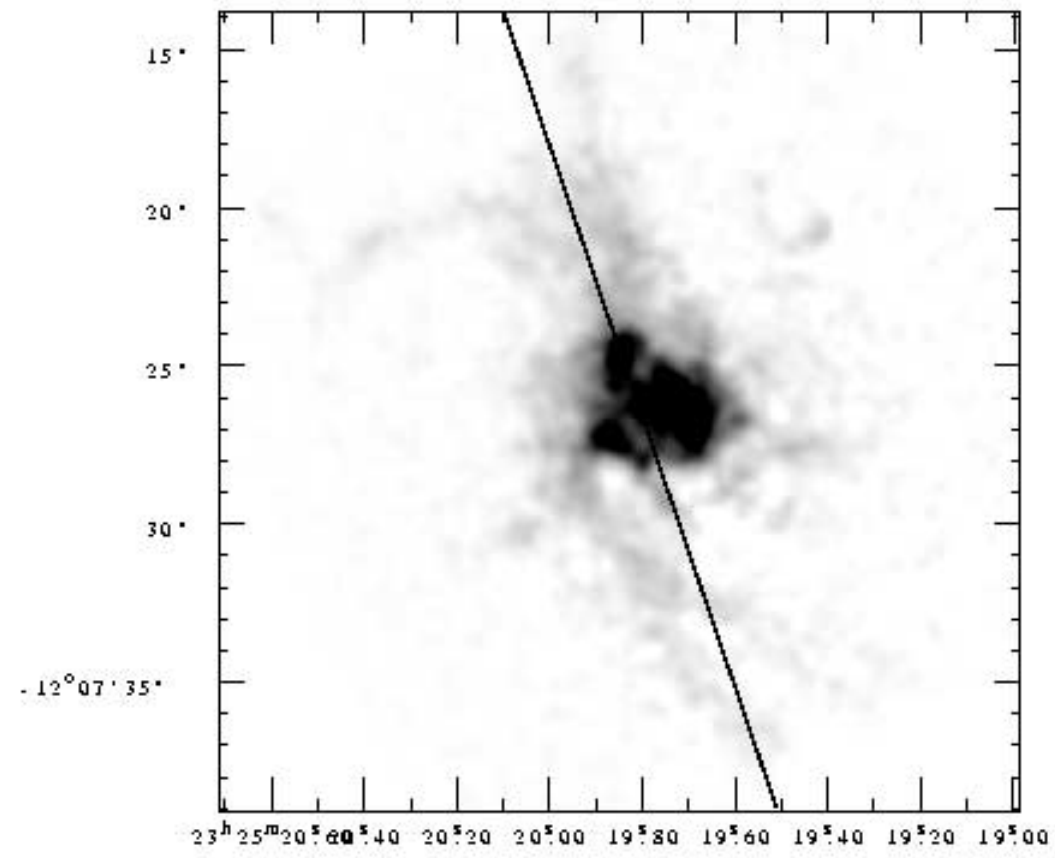

FIG. 3.—A2597: STIS FUV-MAMA Lyα image (O'Dea et al. 2004), showing the location of the slit position angle (19°). Positions are epoch J2000.0.

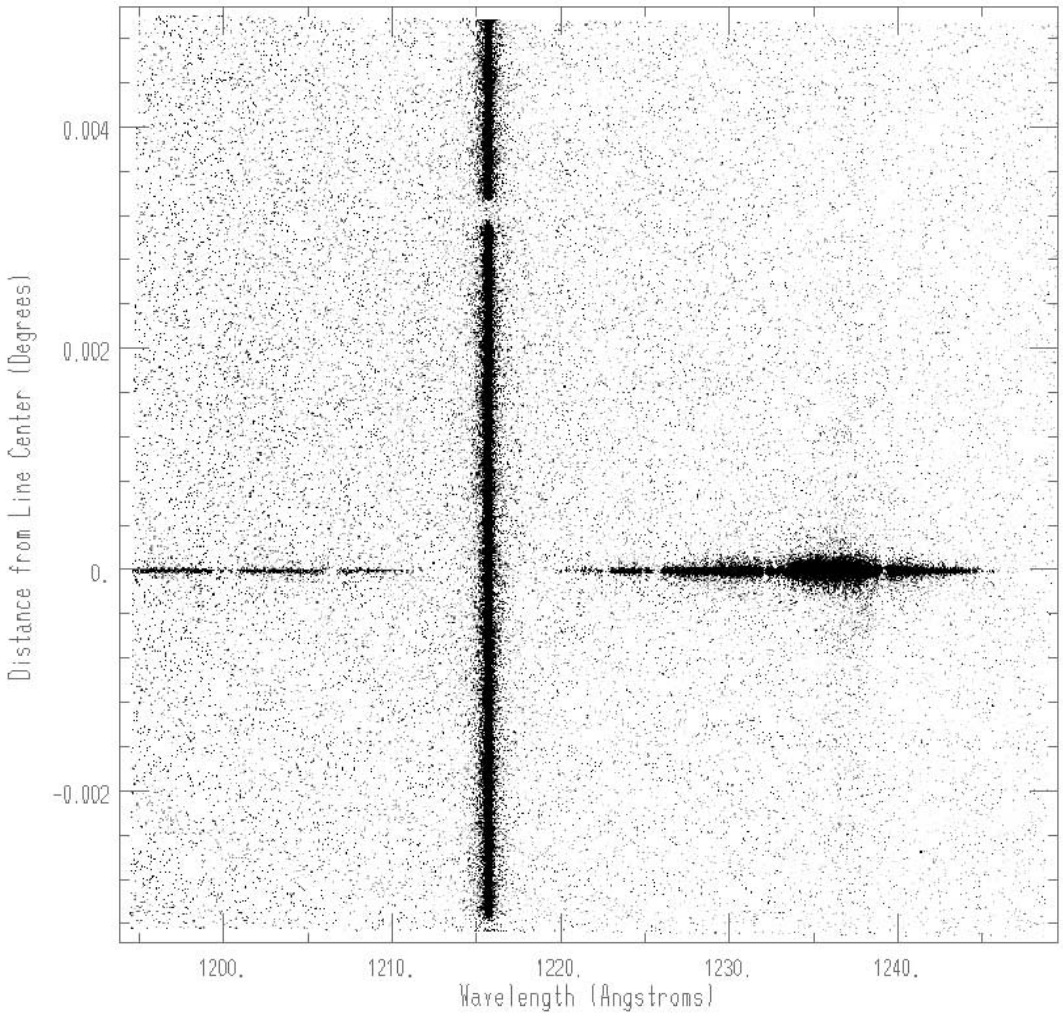

FIG. 4.—A426: Gray-scale image of the STIS FUV-MAMA two-dimensional spectrum. Geocoronal Lyα is visible at 1216 Å. Extended Lyα emission is seen at 1237 Å.

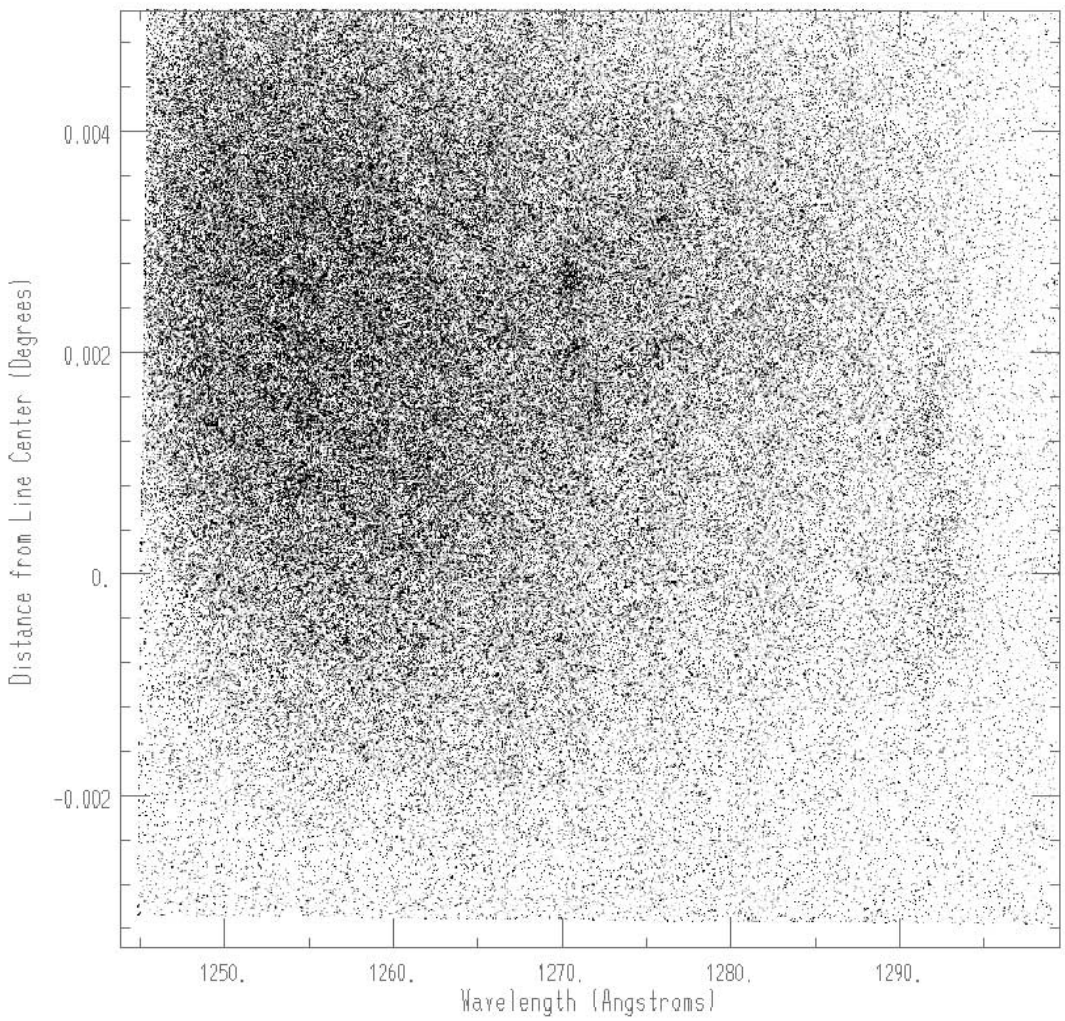

FIG. 5.—A1795: Gray-scale image of the STIS FUV-MAMA two-dimensional spectrum. The background is dominated by a nonuniform glow from the detector window. Faint extended Lyα emission in A1795 is seen at 1292 Å.

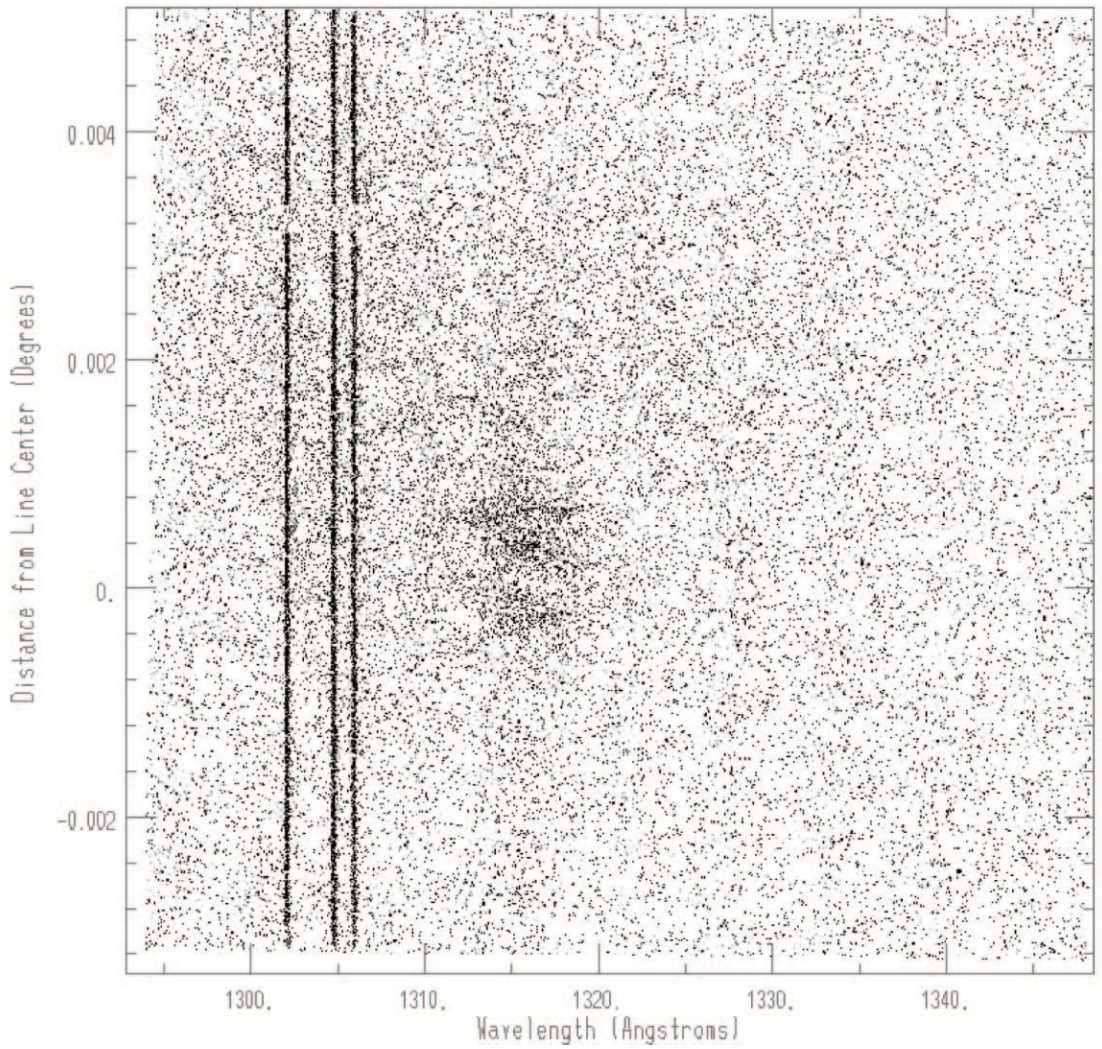

FIG. 6.—A2597: Gray-scale image of the STIS FUV-MAMA two-dimensional spectrum. We detect the O I geocoronal lines at 1302.04, 1304.73, and 1305.90 Å. See Table 3. Faint extended Lyα emission in A2597 is seen at 1316 Å.

The Lyα in NGC 1275 is viewed through two damped Lyα absorption systems, one in our Galaxy at $v = 0$ and one in the infalling high-velocity system ($v = 8200$ km s^{-1}). The data corrected for the effects of these two systems are shown in Figure 8. We estimate column densities of $\sim 1 \times 10^{21}$ cm^{-2} in the damped systems, which is in agreement with the observed 21 cm columns, providing a consistency check on our analysis.

We detect Lyα absorption (feature 8) at the systemic velocity of NGC 1275. However, it is the weakest of our detections. The other absorption features are seen mainly in the wings of the Lyα emission line. Seven of nine features are blueshifted with respect to the systemic velocity of NGC 1275. The absorption systems extend out to -3500 km s^{-1} with respect to systemic.

TABLE 3
GEOCORONAL OXYGEN LINES

Central λ (Å)	Flux (ergs s^{-1} cm^{-2} arcsec^{-2})
1302.04.....	2.938E−12
1304.73.....	2.974E−12
1305.904.....	2.093E−12

NOTES.—Observed wavelength and integrated flux of the geocoronal oxygen lines detected in the G140M spectrum of A2597 (see Fig. 6). The spectra were summed 10″ along the slit.

3.1. *Where Are the Nuclear* 21 cm *Absorbers?*

The 21 cm line has been detected in absorption toward the nucleus of NGC 1275 (Crane et al. 1982; Jaffe 1990; Sijbring 1993) with an optical depth $\tau \simeq 0.0024$ and FWHM ~ 440 km s^{-1}, which gives a column density of $N(\mathrm{H\,I}) \simeq 2 \times 10^{20}$ cm^{-2} for "warm" clouds ($T = 100$ K). However, the column measured in the Lyα absorption line (system 8) is only $N(\mathrm{H\,I}) \simeq 3 \times 10^{12}$ cm^{-2}. This difference suggests that the atomic hydrogen detected in the 21 cm line avoids the line of sight to the nucleus. NGC 1275 exhibits a two-sided (but asymmetric) parsec-scale radio source (e.g., Walker et al. 1994; Vermeulen et al. 1994). Our results imply that the 21 cm absorption is seen against the parsec-scale radio source, but not directly against the Lyα-emitting region in the nucleus.

Multifrequency VLBI observations have shown that there is free-free absorption toward the northern radio jet (e.g., Walker et al. 1994, 2000; Vermeulen et al. 1994). The free-free absorbing medium seems likely to be located in a disk or torus (e.g., Levinson et al. 1995; Walker et al. 2000). We suggest that the

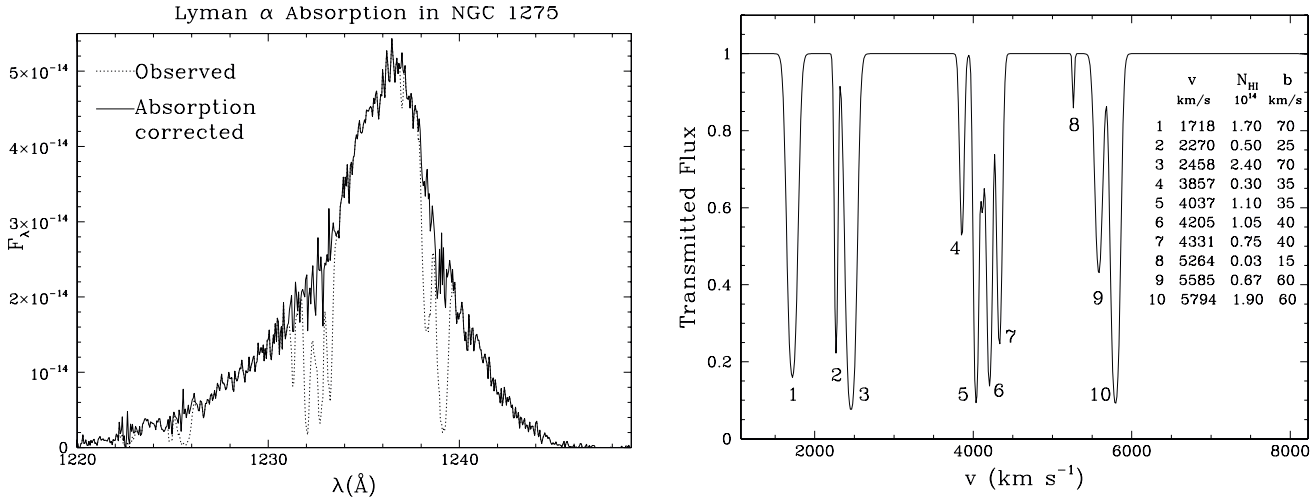

FIG. 7.—A426. *Left*: Observed and absorption-corrected Lyα profile of NGC 1275. The spectrum is integrated in the cross-slit direction since the light distribution is consistent with a point-source emission. *Right*: Fraction of transmitted flux vs. observer-frame velocity. The table on the right lists the parameters of the 10 absorption systems detected, including the central velocity, total H I column, and Doppler *b* parameter. Our 3 σ limit on column density is 1×10^{12} cm^{-2}.

atomic hydrogen responsible for the 21 cm absorption may also be located in that putative disk or torus.

3.2. *Comparison of the STIS and FOS Spectra at Similar Resolution*

Johnstone & Fabian (1995) presented an *HST* FOS spectrum of the nucleus of NGC 1275 taken 1993 February 3 through the G130H grating with a spectral resolution of ∼1 Å. They found an apparent dip in the spectrum at 1237 Å, which they attributed to the presence of a blueshifted component of Lyα produced by Fermi-accelerated Lyα emission (Neufeld & McKee 1988; Binette et al. 1998). For NGC 1275, this model requires that the Lyα photons be scattered back and forth across a shock with velocity $v_s \sim 100$ km s^{-1} and atomic hydrogen column density 1.1×10^{20} cm$^{-2} < N < 1.3\times10^{21}$ cm^{-2} (Johnstone & Fabian 1995). The Lyα photons must also be generated in or near the shock to avoid destruction by dust associated with these high columns.

In Figure 9 we present a comparison of the FOS 130H data with our STIS G140M spectrum scaled to similar spectral resolution. The FOS spectrum has too low resolution and too low signal-to-noise ratio to have detected the 10 Lyα absorption features that we detect in our STIS G140M spectrum. However, we should have seen the feature in the FOS spectrum at 1237 Å. The discrepancy could be due to bad data in the FOS spectrum. However, it is also possible that the 1237 Å feature is variable. This would imply that it is an "intrinsic absorption feature" (see § 3.3.1). If the variability of the feature is due to the motion of clouds near the nucleus, at a velocity of 0.01*c* perpendicular to our line of sight, they could move only 0.07 lt-yr in the ∼7 yr between the two observations. Thus, the clouds should be less than 0.025 pc across. Alternately, the difference in the STIS and FOS spectra could be at least partially due to aperture affects. The larger FOS aperture contains a contribution from extended Lyα emission that exhibits a Lyα absorption feature at the systemic velocity (see below). This could be the source of the feature seen in the FOS spectrum.

TABLE 4
ABSORPTION LINES DETECTED TOWARD NGC 1275

Feature (1)	EW (Å) (2)	λ (Å) (3)	*v* (km s^{-1}) (4)	*N*(H) (10^{14} cm^{-2}) (5)	*b* (km s^{-1}) (6)
1	0.5383	1223	1718	1.70	70
2	0.1715	1225	2270	0.50	25
3	0.6398	1226	2458	2.40	70
4	0.1331	1231	3857	0.30	35
5	0.3093	1232	4037	1.10	35
6	0.3232	1233	4205	1.05	40
7	0.2666	1233	4331	0.75	40
8	0.1567E−01	1237	5264	0.03	15
8[a]	...	1237	5264	0.80	80
9	0.2817	1238	5585	0.67	60
10	0.5348	1239	5794	1.90	60
11[a, b]	...	1237	5259	...	...

NOTES.—Properties of the detected absorption lines. Col. (1): Assigned number; col. (2): equivalent width; col. (3): observed central wavelength of the line; col. (4): heliocentric velocity of the line; col. (5): estimated column density of atomic hydrogen, assuming a covering factor of unity; col. (6): Doppler *b* factor (where $b = \sigma\sqrt{2}$ and σ is the Gaussian dispersion).

[a] Detected toward the extended emission.

[b] Uncertain detection.

3.3. *What Are the Absorption Features toward NGC 1275?*

3.3.1. *Intrinsic Nuclear Absorption Features*

Seven of nine features seen toward the nucleus of NGC 1275 are blueshifted with respect to the systemic velocity of NGC 1275. The absorption systems extend out to −3500 km s^{-1} with respect to systemic. One possibility that applies to these systems is that they are associated with outflowing nuclear gas. We note that "intrinsic" absorption features are found in about half of Seyfert I AGNs (e.g., Crenshaw et al. 1999), which have optical and X-ray luminosity similar to NGC 1275. The intrinsic absorption features in AGNs tend to be blueshifted, variable, have a range of line widths of ∼20−400 km s^{-1}, and exhibit high-ionization metal lines (e.g., Weymann et al. 1997; Crenshaw et al. 1999; Kriss et al. 2000). The intrinsic features are thought to be produced by clouds in an outflowing wind.

The column densities, widths, and velocity offsets of the absorption features in NGC 1275 are roughly consistent with those of intrinsic absorption features. In addition, the possibility that the 1237 Å feature (if real) is variable is also consistent with that

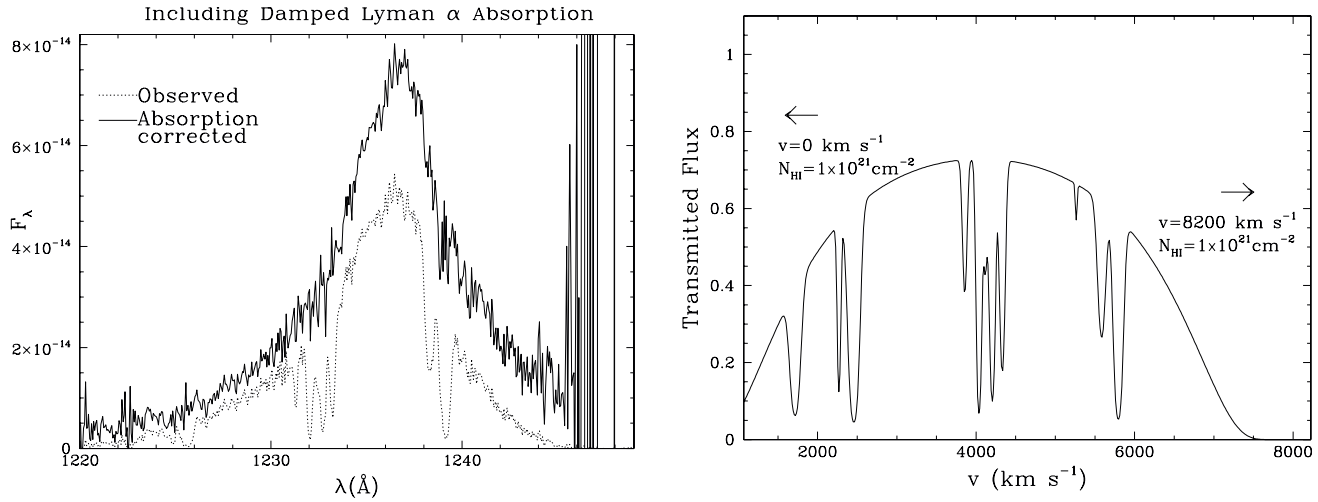

FIG. 8.—A426: Same as Fig. 7, but including corrections for damped Lyα absorption by the Galaxy (at $v = 0$) and by the foreground infalling galaxy (at $v = 8200$ km s^{-1}). The Lyα absorption profile of both systems suggests a column of about 1×10^{21} cm^{-2}, consistent with the 21 cm absorption by these systems.

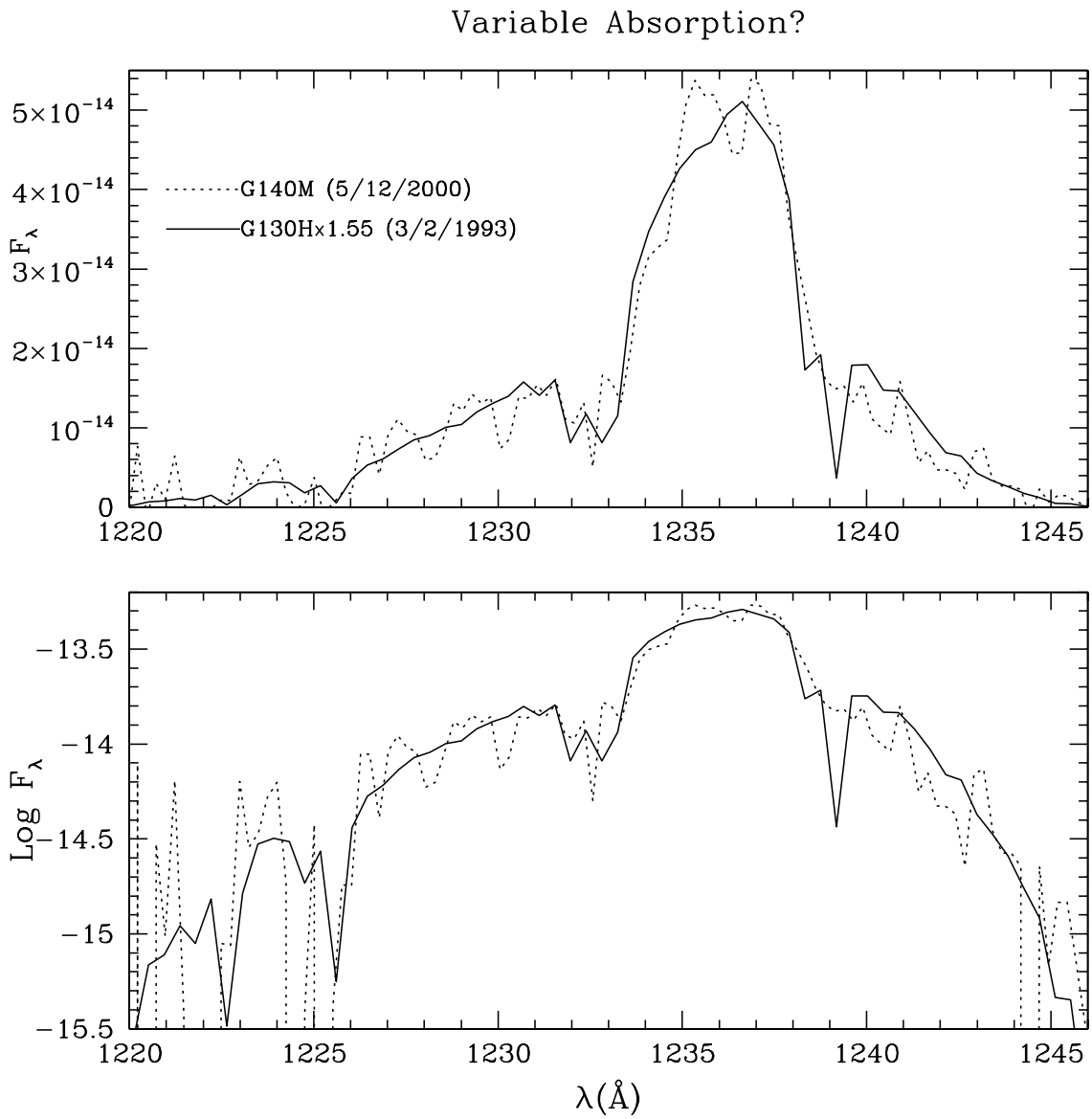

FIG. 9.—A426: Comparison of the 1993 FOS G130H spectrum (Johnstone & Fabian 1995) with our 2000 STIS G140M spectrum. The FOS spectrum was scaled by a factor of 1.55 to match the STIS spectrum. The STIS G140M spectrum has been rebinned by a factor of 8 (pixel size 0.85 Å) so that it has resolution similar to that of the FOS G130H spectrum.

TABLE 5
CANDIDATE IDENTIFICATIONS

Feature (1)	Galaxy (2)	Type (3)	Magnitude (4)	$V_{\rm line} - V_{\rm ID}$ (km s^{-1}) (5)	Offset (arcsec) (6)	Offset (kpc) (7)
4.....	Per 152	E	15	−80	203	67
4.....	PGC 012423	E	17	−106	238	79
5.....	PGC 012423	E	17	74	238	79
9.....	PGC 012441	E	16	99	94	31
10.....	PGC 012433	E?	18	−27	92	31

NOTES.—Results from a NED search using $V = 1000$–6000 km s^{-1} within a box $8'$ across, centered on NGC 1275. There are two candidate identifications for feature 4. Col. (1): Number of the absorption feature (see Table 4); col. (2): name of the galaxy that is a candidate for identification with the absorption line; col. (3): Hubble type of the galaxy; col. (4): magnitude of the candidate galaxy; col. (5): offset in velocity between the absorption line and the candidate galaxy; col. (6): angular separation between the candidate galaxy and the nucleus of NGC 1275; col. (7): offset in kpc, assuming the system is at the distance of the Perseus Cluster.

origin. Additional observations to search for variability and determine the metalicity of the systems would test this scenario.

3.3.2. *Emission-Line Filaments*

We have compared the velocities of the absorption features with those of the emission-line filaments given by Conselice et al. (2001). The emission-line filaments cover a velocity range of roughly 5000–5500 km s^{-1}. We find that only one absorption feature (system 8) agrees with the velocity of any of the filaments. In fact, most of the absorption features lie at velocities well beyond the range of velocities of the emission-line filaments. Thus, the emission-line filaments do not produce the majority of the absorption features.

The radio source 3C 84 appears to have evacuated "bubbles" in the ICM (e.g., Böhringer et al. 1993; McNamara et al. 1996; Fabian et al. 2000). A. C. Fabian (2003, private communication) has noted that we may be viewing the nucleus of NGC 1275 through the northern bubble and has suggested that the bubble has displaced the emission-line filaments from our line of sight to the nucleus. An alternate possibility is that any dense line-emitting clouds that have been engulfed by the expanding bubble have been destroyed by shredding (e.g., Loewenstein & Fabian 1990; Klein et al. 1994; O'Dea et al. 2003, 2004).

3.3.3. *Galaxies in the Perseus Cluster*

We have searched in NED for galaxies close to NGC 1275 in projection and in velocity that might be candidates for some of the absorption features (Table 5). We searched a box-shaped region $8'$ across centered on NGC 1275 and within a heliocentric velocity range 1000–6000 km s^{-1}. We find that four of the absorption systems have potential associations with cluster galaxies 30–80 kpc in projection to the line of sight and 27–106 km s^{-1} offset in velocity. At this point it is not clear which if any of these candidate associations are real.

3.3.4. Lyα *Forest Systems*

The column densities and Doppler b parameters of the absorption features toward NGC 1275 are similar to those of typical Lyα forest systems (e.g., Rauch 1998). However, according to Bahcall et al. (1996), the density of the Lyα forest at $z \sim 0$ is $dN/dz = 24.5 \pm 6.6$ for systems with EW > 0.25 Å. Now, the 10 absorption systems we see cover $\Delta v = 4076$ km s^{-1}, or $dz = \Delta v/c = 0.0136$. Thus, we would have expected $0.0136 \times 24.5 = 0.33$ Lyα forest systems to fall at the velocity interval we observed, while there are 7 (out of the 10) systems with EW > 0.25 Å. So, this suggests that the systems we have detected are most likely not part of the general Lyα forest in the direction of A426. Since the velocity range of the Lyα absorption systems is so much larger than the velocity range of the Hα emission filaments (Conselice et al. 2001), it seems that the best bet is that most of these absorption systems are associated with the active nucleus.

4. CONSTRAINTS ON EXTENDED ABSORPTION IN A426, A1795, AND A2597

Figure 10 shows a comparison of the nuclear spectrum with the sum of two off-nuclear emission regions. We detect the absorption system seen against the nucleus at the systemic velocity of 5264 km s^{-1} and possibly also a system at 5259 km s^{-1}, which is not formally detected against the nucleus. The column density in the extended 5264 km s^{-1} system is about a factor of 30 times larger than that seen toward the nucleus. This suggests that the extended absorbing system is possibly associated with the plane of the galaxy. If the extended system is damped and is seen with an absorption depth of 0.5 because of scattering or partial covering, then the upper limit to the estimated column becomes $N({\rm H\,I}) < 2 \times 10^{18}$ cm^{-2}.

Extracted spectra showing Gaussian fits to the extended Lyα emission lines in A1795 and A2597 are shown in Figures 11 and 12. The results of the Gaussian fits are presented in Table 6.

A fairly conservative upper limit on the absorption EW in these spectra is 0.1 Å, or 25 km s^{-1}. We use the curve of growth analysis in Laor (1997) to convert the EW to a column density. Laor gives convenient analytic approximations for the three regimes in the curve of growth (linear, saturated, and damped). When the absorption becomes optically thick, the absorption EW $\simeq 1.66b$, so the optically thin case applies for EW $= 0.1$ Å when $b > 15$ km s^{-1}, and in that regime $N({\rm H\,I}) \simeq 1.8 \times 10^{13}$ cm^{-2}. The transition to damped absorption occurs when $b < 4$ km s^{-1}, which happens when $T < 10^3$ K, and in that case $N({\rm H\,I}) \simeq 5.9 \times 10^{16}$ cm^{-2}. We suspect that such cold and kinematically quiet H I inside clusters is quite unlikely, so the $b > 15$ km s^{-1} H I column estimate is probably much more realistic. Thus, we find an implied column density of $\lesssim 10^{13}$ cm^{-2} if the Doppler parameter $b > 13$ km s^{-1}.

Alternately, the covering factor of any high column density gas must be less than ~25%. We note that in PKS 2322−123, the extended 21 cm absorption is consistent with a covering factor as low as 6×10^{-3} (O'Dea et al. 1994).

5. IMPLICATIONS

Many mechanisms have been proposed to explain the lack of cooling gas below temperatures of about 1 keV in "cooling

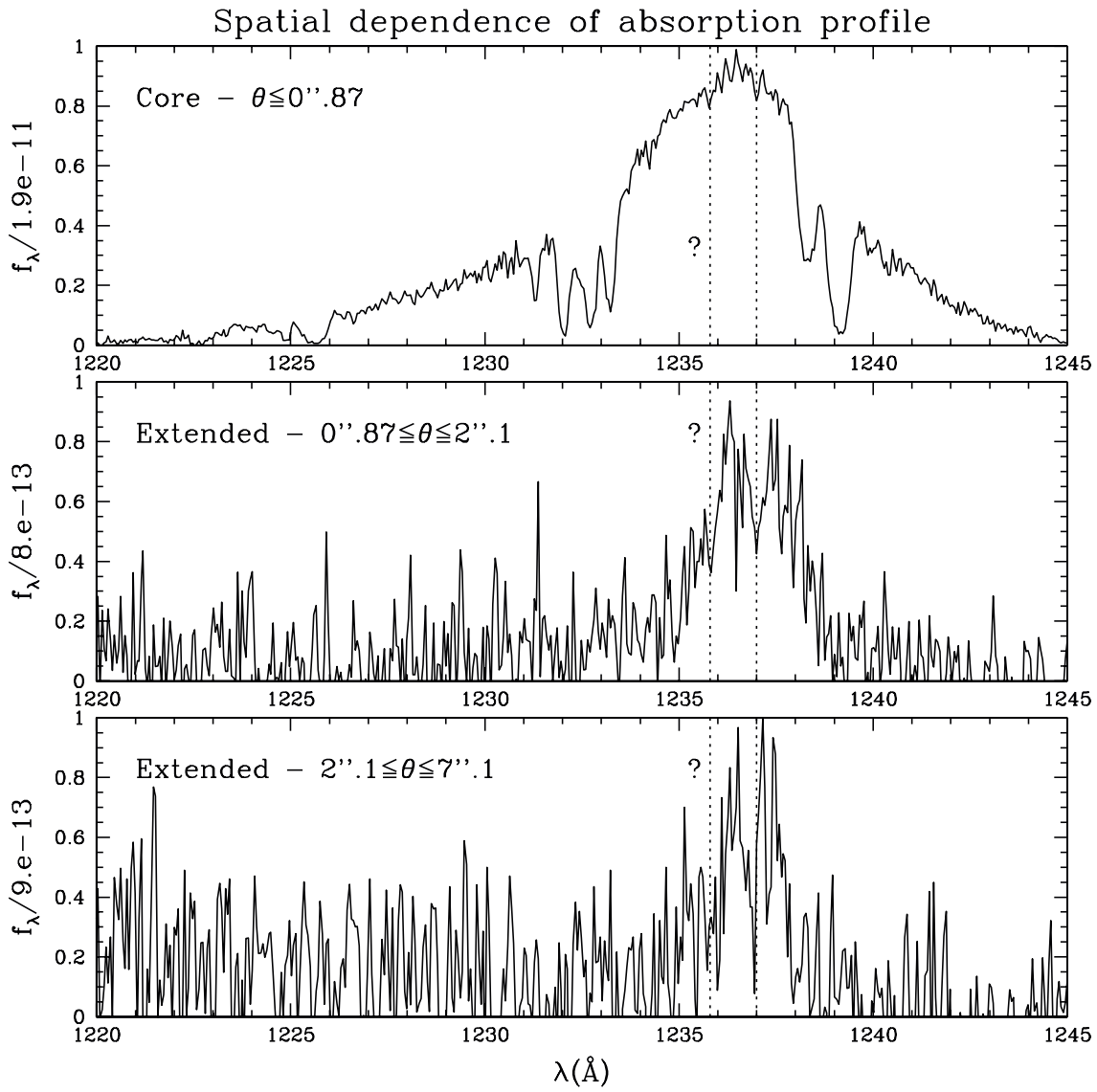

FIG. 10.—A426: G140 spectra. *Top*, Nucleus of NGC 1275; *middle*, sum of extended emission between 0″.87 and 2″.1 from the nucleus; *bottom*, sum of extended emission between 2″.1 and 7″.1 from the nucleus.

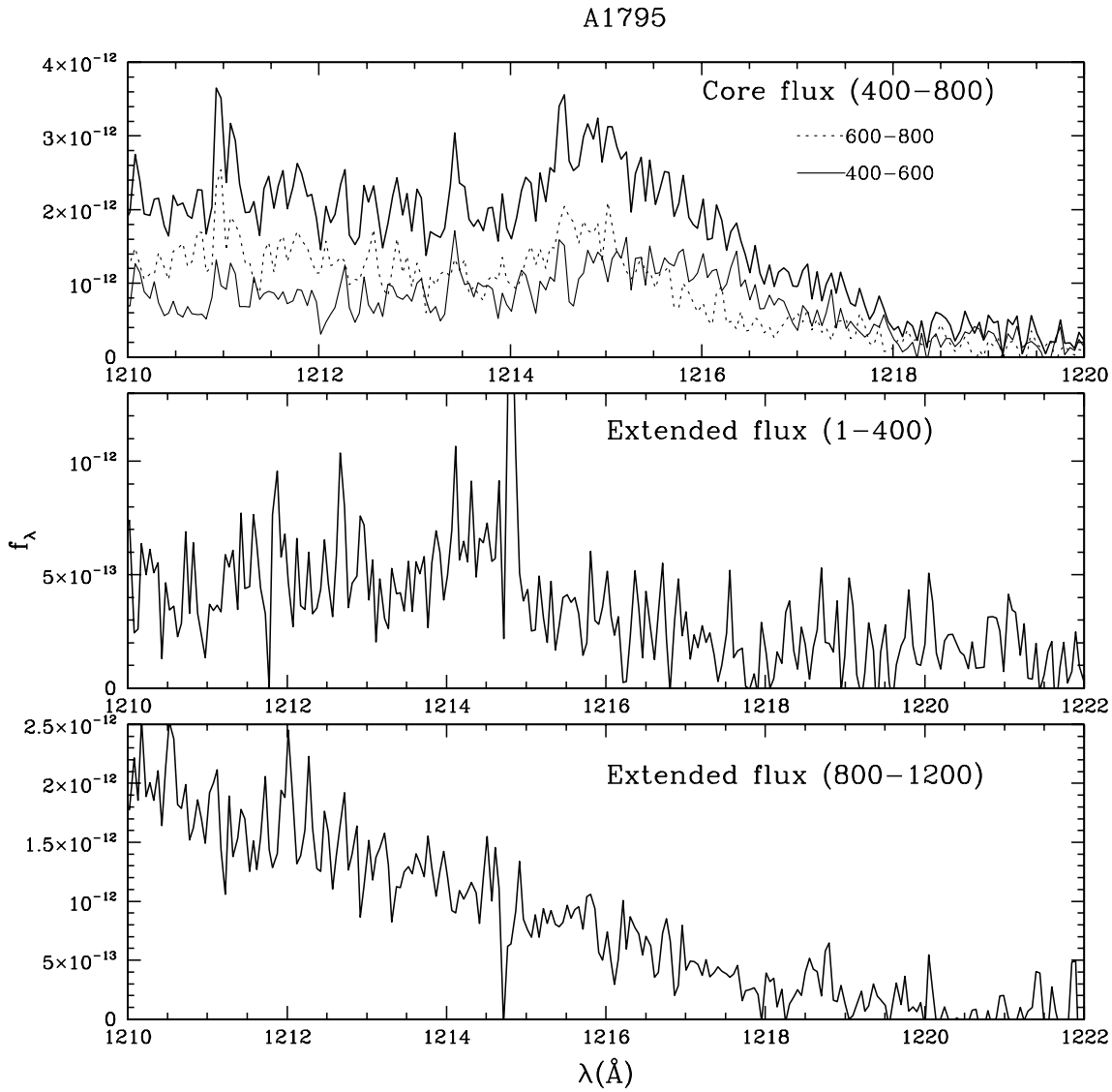

FIG. 11.—A1795: G140 spectra vs. rest wavelength. Each panel shows a spectrum integrated along 1/3 of the slit, corresponding to 11″.6 (row numbers are indicated in parentheses, where row 1 corresponds to the bottom of the image in Fig. 5, south). Significant Lyα emission is detected near the core. The peak of the emission from the upper half of the core (rows 600–800) is blueshifted by $\sim$200 km s^{-1} compared to the emission from the lower half (rows 400–600). Some extended emission may be present south of the nucleus region, but none is detected to the north. The apparent rise in the spectrum in the south results from a nonuniform instrumental background. No clear Lyα absorption is present toward the nucleus.

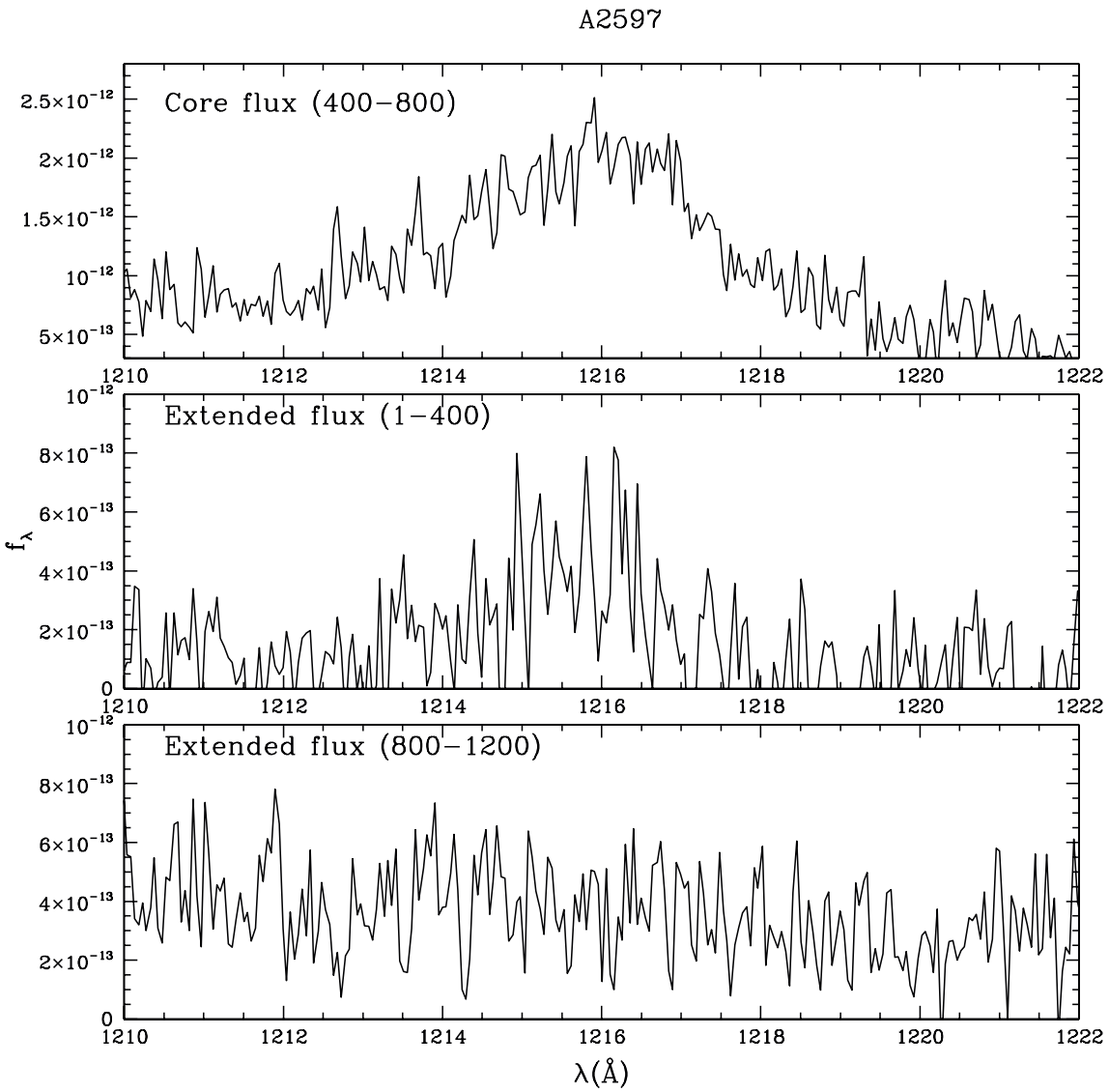

FIG. 12.—A2597: Same as Fig. 11, but for A2597. Extended emission is present to the south, but none to the north. No clear Lyα absorption is present toward the nucleus.

flow'' clusters (e.g., Peterson et al. 2001; Fabian et al. 2001). Our results are relevant to models that invoke differential absorption by cold gas to hide the missing low-temperature X-ray gas. Fabian et al. estimate that the required atomic hydrogen column densities are in the range of a few times 10^{21}–10^{22} cm^{-2}. Such high columns would have been easily seen in Lyα absorption, since our upper limits are of the order of $\sim 10^{13}$ cm^{-2}. The covering factors would need to be fairly high in order to reduce the emission from the cooling gas by the observed factors of 5–10 (e.g., Peterson et al. 2003). Fabian et al. note that the cold gas need not have a uniform distribution in the ICM, but must preferentially cover the regions where gas is cooling. Since our observations sample the lines of sight to the emission-line nebula (which are presumably the locations of the cooling gas), we directly constrain this reduced covering factor model. Thus, we find that the ''missing'' cooling gas in cooling core clusters is unlikely to be hidden by absorption.

TABLE 6
PROPERTIES OF THE EXTENDED Lyα EMISSION

Galaxy	Slit Length (arcsec)	Flux (ergs s^{-1} cm^{-2})	Central λ (Å)	FWHM (Å)	FWHM (km s^{-1})
A426.....	5.8	2.4×10^{-12}	1236.67	3.2	780
A1795.....	12.9	4.9×10^{-12}	1291.80	2.7	630
A2597.....	18.7	6.8×10^{-12}	1315.79	3.7	844

NOTES.—The results of Gaussian fits to the spectra. The slit length is the distance along the slit that was summed to produce the spectrum.

More generally, we place limits on the column density of cool gas along our line of sight to the bright central emission-line nebulae. Thus, our results constrain the amount of cool gas embedded in the hot ICM, i.e., outside the dense nebulae in the central $\sim$10–20 kpc of the cluster (e.g., Edge 2001; Jaffe et al. 2005). If we assume that absorption feature 10 is one such system in the ICM, the column density of 2×10^{14} cm^{-2} implies a total mass of $\sim$40,000 $M_\odot$ of cold gas in the hot ICM within a shell of radius $\sim$20–100 kpc. If dense cold gas is injected into the ICM, e.g., by ram pressure stripping from galaxies (e.g., Soker et al. 1991) or cooling on the $\sim$100 kpc scale, it can sink to the center of the cluster on a timescale no shorter than $\sim$(100 kpc)/(1000 km s^{-1}) $\sim 10^8$ yr. This limits the rate at

which cold gas can accumulate in the ICM on 100 kpc scales. The accumulation rate (i.e., the difference between the sources and sinks of cold gas) is constrained to be no more than about $4\times10^{-4}\ M_\odot\ \mathrm{yr}^{-1}$. This suggests that (1) if cold clouds are not efficiently destroyed, injection of cold gas into the hot ICM (by any mechanism, including cooling) on 100 kpc scales is very low, $\sim10^{-4}\ M_\odot\ \mathrm{yr}^{-1}$, or (2) any cold clouds on 100 kpc scales are efficiently reheated or destroyed (e.g., Loewenstein & Fabian 1990), and (3) the dense nebulae in the cluster center are produced by gas that is deposited or that cools in situ.

6. SUMMARY

We present *HST* STIS long-slit spectroscopy of the Lyα line in A426, A1795, and A2597. We detect 10 Lyα absorption systems toward the nucleus of NGC 1275 with estimated column densities in the range $N(\mathrm{H\,I})\sim10^{12}$–$10^{14}\ \mathrm{cm}^{-2}$. These systems could not have been detected in the 21 cm line, but are easily detected in Lyα absorption. Most of the detected features are located in the broad wings of the emission line and are beyond the velocity range of the emission-line filaments. The detected absorption systems are most consistent with associated nuclear absorption systems. Further observations of variability and/or the metal lines are necessary to confirm this hypothesis.

We do not detect the feature at 1237 Å reported by Johnstone & Fabian (1995) and interpreted as being due to Fermi-accelerated Lyα. If real, this feature is variable and would be consistent with an intrinsic absorbing system.

There is very little absorption at the systemic velocity of NGC 1275 [feature 8 contains $N(\mathrm{H\,I})\sim3\times10^{12}\ \mathrm{cm}^{-2}$]. This implies that the very large column densities detected in the 21 cm line avoid the line of sight to the nuclear Lyα-emitting region and are likely detected against the parsec-scale radio jet. This atomic gas may be located in a circumnuclear disk or torus.

We detect two absorption systems (one at the systemic velocity) toward the extended Lyα emission in A426. We do not detect Lyα absorption toward the extended diffuse Lyα emission in A1795 and A2597, with upper limits $N(\mathrm{H\,I})\lesssim10^{13}\ \mathrm{cm}^{-2}$ for optically thin absorbers with unity covering factor. Alternately, our data constrain the covering factor of any high column density gas [$N(\mathrm{H\,I})\gtrsim10^{15}\ \mathrm{cm}^{-2}$] to be less than 25%.

Our results suggest that it is unlikely that the "missing" gas at temperatures below 1 keV in the cooling cores is due to absorption by large columns of absorbing gas with a covering factor of order unity. In addition, the low columns of gas on $\sim$100 kpc scales in the ICM suggests that (1) the rate at which cold gas accumulates in the ICM on these scales is very low and (2) the dense nebulae in the central $\sim$10 kpc must have cooled or been deposited in situ.

We are grateful to Andy Fabian, Jerry Kriss, and Rajib Ganguly for helpful discussions. We thank the anonymous referee for helpful comments. Support for program 8107 was provided by NASA through a grant from the Space Telescope Science Institute, which is operated by the Association of Universities for Research in Astronomy, Inc., under NASA contract NAS 5-26555. This research made use of (1) the NASA/IPAC Extragalactic Database (NED), which is operated by the Jet Propulsion Laboratory, California Institute of Technology, under contract with the National Aeronautics and Space Administration and (2) NASA's Astrophysics Data System Abstract Service.

REFERENCES

Allen, R. J., Knapen, J. H., Bohlin, R., & Stecher, T. P. 1997, ApJ, 487, 171
Allen, S. W. 1995, MNRAS, 276, 947
Allen, S. W., & Fabian, A. C. 1994, MNRAS, 269, 409
Allen, S. W., Fabian, A. C., Johnstone, R. M., White, D. A., Daines, S. J., Edge, A. C., & Stewart, G. C. 1993, MNRAS, 262, 901
Bahcall, J. N., & Ekers, R. D. 1969, ApJ, 157, 1055
Bahcall, J. N., et al. 1996, ApJ, 457, 19
Baum, S. A., & O'Dea, C. P. 1991, MNRAS, 250, 737
Binette, L., Joguet, B., & Wang, J. C. L. 1998, ApJ, 505, 634
Blanton, E. L., Sarzain, C. L., & McNamara, B. R. 2003, ApJ, 585, 227
Böhringer, H., & Fabian, A. C. 1989, MNRAS, 237, 1147
Böhringer, H., Matsushita, K., Churazov, E., Ikebe, Y., & Chen, Y. 2002, A&A, 382, 804
Böhringer, H., Voges, W., Fabian, A. C., Edge, A. C., & Neumann, D. M. 1993, MNRAS, 264, L25
Boselli, A., Lequeux, J., & Gavazzi, G. 2002, A&A, 384, 33
Burns, J. O., White, R. A., & Haynes, M. P. 1981, AJ, 86, 1120
Conselice, C. J., Gallagher, J. S., & Wyse, R. F. G. 2001, AJ, 122, 2281
Cowie, L. L., & Binney, J. 1977, ApJ, 215, 723
Crane, P. C., van der Hulst, J. M., & Haschick, A. D. 1982, in IAU Symp. 97, Extragalactic Radio Sources, ed. D. S. Heeschen & C. M. Wade (Dordrecht: Reidel), 307
Crawford, C. S., Fabian, A. C., Johnstone, R. M., & Crehan, D. A. 1987, MNRAS, 224, 1007
Crenshaw, D. M., Kraemer, S. B., Boggess, A., Maran, S. P., Mushotzky, R. F., & Wu, C.-C. 1999, ApJ, 516, 750
Dwarakanath, K. S., van Gorkom, J. H., & Owen, F. N. 1994, ApJ, 432, 469
Edge, A. C. 2001, MNRAS, 328, 762
Ettori, S., Fabian, A. C., Allen, S. W., & Johnstone, R. M. 2002, MNRAS, 331, 635
Fabian, A. C. 1994, ARA&A, 32, 277
Fabian, A. C., Allen, S. W., Crawford, C. S., Johnstone, R. M., Morris, R. G., Sanders, J. S., & Schmidt, R. W. 2002, MNRAS, 332, L50
Fabian, A. C., Mushotzky, R. F., Nulsen, P. E. J., & Peterson, J. R. 2001, MNRAS, 321, L20
Fabian, A. C., & Nulsen, P. E. J. 1977, MNRAS, 180, 479
Fabian, A. C., et al. 2000, MNRAS, 318, L65
Hu, E. M., Cowie, L. L., & Wang, Z. 1985, ApJS, 59, 447
Jaffe, W. 1990, A&A, 240, 254
———. 1991, A&A, 250, 67
———. 1992, in Clusters and Superclusters of Galaxies, ed. A. C. Fabian (NATO ASI Ser. C, 366; Dordrecht: Kluwer), 109
Jaffe, W., Bremer, M. N., & Baker, K. 2005, MNRAS, 360, 748
Johnstone, R. M., & Fabian, A. C. 1995, MNRAS, 273, 625
Kaastra, J. S., Ferrigno, C., Tamura, T., Paerels, F. B. S., Peterson, J. R., & Mittaz, J. P. D. 2001, A&A, 365, 99L
Kaastra, J. S., et al. 2004, A&A, 413, 415
Kent, S. M., & Sargent, W. L. W. 1979, ApJ, 230, 667
Kimble, R. A., et al. 1998, ApJ, 492, L83
Klein, R., McKee, C., & Colella, P. 1994, ApJ, 420, 213
Koekemoer, A. M., O'Dea, C. P., Baum, S. A., Sarazin, C. L., Owen, F. N., & Ledlow, M. J. 1998, ApJ, 508, 608
Kriss, G. A., et al. 2000, ApJ, 538, L17
Laor, A. 1997, ApJ, 483, L103
Levinson, A., Laor, A., & Vermeulen, R. C. 1995, ApJ, 448, 589
Loewenstein, M., & Fabian, A. C. 1990, MNRAS, 242, 120
Mathews, W. G., & Bregman, J. N. 1978, ApJ, 224, 308
McNamara, B. R., Bregman, J., N., & O'Connell, R. W. 1990, ApJ, 360, 20
McNamara, B. R., O'Connell, R. W., & Sarazin, C. L. 1996, AJ, 112, 91
Miller, E. D., Bregman, J. N., & Knezek, P. M. 2002, ApJ, 569, 134
Mushotzky, R. F. 1992, in Clusters and Superclusters of Galaxies, ed. A. C. Fabian (NATO ASI Ser. C, 366; Dordrecht: Kluwer), 91
Neufeld, D. A., & McKee, C. F. 1988, ApJ, 331, L87
O'Dea, C. P., Baum, S. A., & Gallimore, J. F. 1994, ApJ, 436, 669
O'Dea, C. P., Baum, S. A., Mack, J., Koekemoer, A., & Laor, A. 2004, ApJ, 612, 131
O'Dea, C. P., Gallimore, J. F., & Baum, S. A. 1995, AJ, 109, 26
O'Dea, C. P., Payne, H., & Kocevski, D. 1998, AJ, 116, 623
O'Dea, C. P., et al. 2003, Publ. Astron. Soc. Australia, 20, 88
Peterson, J. R., Kahn, S. M., Paerels, F. B. S., Kaastra, J. S., Tamura, T., Bleeker, J. A. M., Ferrigno, C., & Jernigan, J. G. 2003, ApJ, 590, 207
Peterson, J. R., et al. 2001, A&A, 365, L104
Rauch, M. 1998, ARA&A, 36, 267
Rybicki, G., & Lightman, A. P. 1979, Radiative Processes in Astrophysics (New York: Wiley)

Sarazin, C. L. 1988, X-Ray Emission from Clusters of Galaxies (Cambridge: Cambridge Univ. Press)
Sijbring, D. 1993, Ph.D. thesis, Univ. Groningen
Soker, N., Blanton, E. L., & Sarazin, C. L. 2002, ApJ, 573, 533
Soker, N., Bregman, J. N., & Sarazin, C. L. 1991, ApJ, 368, 341
Sparks, W. B. 1992, ApJ, 399, 66
Sparks, W. B., Macchetto, F. D., & Golombek, D. 1989, ApJ, 345, 153
Tamura, T., et al. 2001, A&A, 365, L87
Taylor, G. B. 1996, ApJ, 470, 394
Taylor, G. B., O'Dea, C. P., Peck, A. B., & Koekemoer, A. M. 1999, ApJ, 512, L27
Tucker, W., & David, L. P. 1997, ApJ, 484, 602
Valentijn, E. A., & Giovanelli, R. 1982, A&A, 114, 208
Vermeulen, R. C., Readhead, A. C. S., & Backer, D. C. 1994, ApJ, 430, L41
Voit, G. M., & Donahue, M. 1997, ApJ, 486, 242
Walker, R. C., Dhawan, V., Romney, J. D., Kellermann, K. I., & Vermeulen, R. C. 2000, ApJ, 530, 233
Walker, R. C., Romney, J. D., & Benson, J. M. 1994, ApJ, 430, L45
Weymann, R. J., Morris, S. L., Gray, M. E., & Hutchings, J. B. 1997, ApJ, 483, 717
White, D. A., Fabian, A. C., Johnstone, R. M., Mushotzky, R. F., & Arnaud, K. A. 1991, MNRAS, 252, 72